Identification of Antiviral Roles for the Exon-Junction Complex and Nonsense-Mediated Decay in Flaviviral Infection

Supplementary Information

Supplementary Figures

Supplementary Figure 1: Expression of WNV bait proteins. Anti-strep western blot of all WNV proteins, and DENV and ZIKV capsid proteins, after transient transfection and affinity purification from HEK293 cells with bait proteins indicated by red arrows. Results are representative of four biologically independent experiments repeated with similar results.

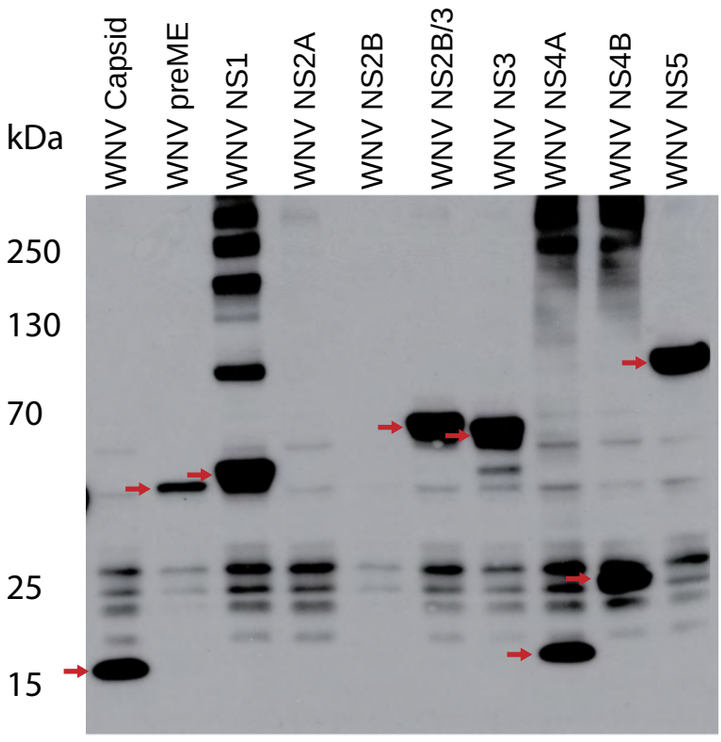

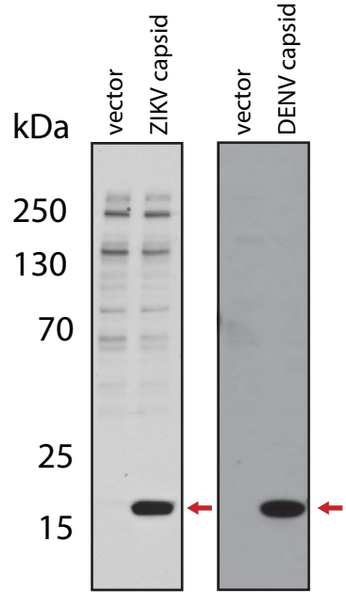

Supplementary Figure 1

Supplementary Figure 2: Abundance of bait proteins detected in each sample. The number of peptides found for each WNV bait protein in each replicate is indicated. The color of each square corresponds to the number of peptides as indicated by the scale at the right. Results were calculated from four biologically independent experiments.

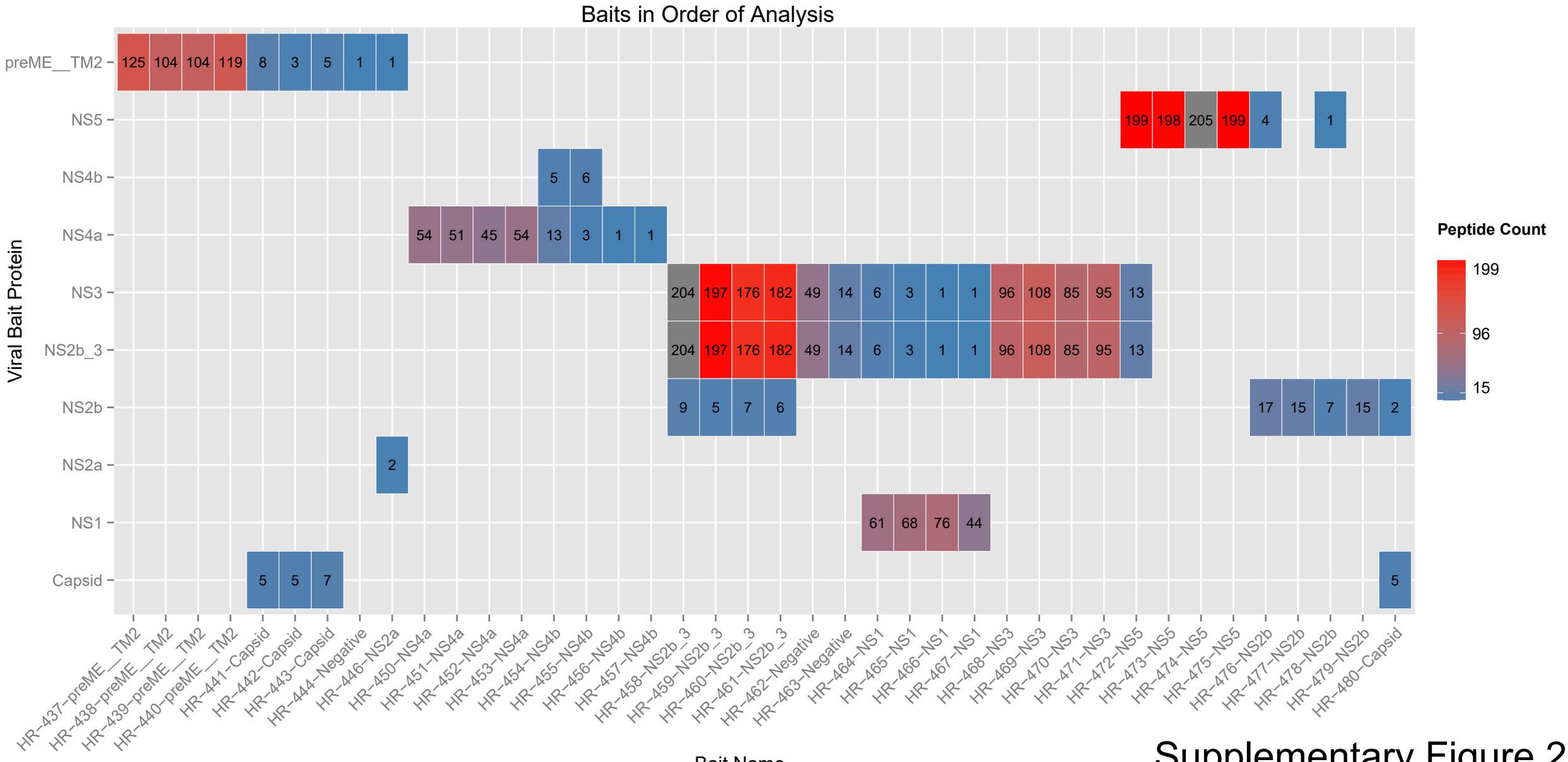

Supplementary Figure 2

Supplementary Figure 3: Conservation of flavivirus NS5 proteins: This table summarizes a pairwise comparison with the percentage of amino acid conservation between flavivirus NS5 proteins.

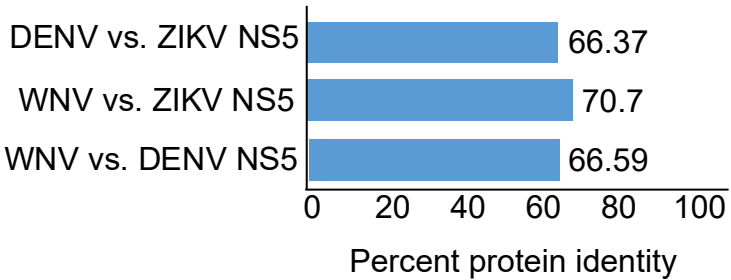

Supplementary Figure 3

Supplementary Figure 4: DDX55 localization and knock-downs. a, Localization of strep-tagged proteins in WNV capsid-strep transfected (upper panel) and untransfected (lower panel) U2OS cells. Strep-tagged protein is shown in green using a Strep tag-specific antibody. Nuclear staining (Hoescht) is shown in blue. **b**, Localization of V5-tagged proteins in DDX55-V5 transfected (upper panel) and untransfected (lower panel) U2OS cells. V5-tagged protein is shown in green using a V5-specific antibody. Nuclear staining is shown in blue**. c**, Localization of native WNV capsid and native DDX55 using specific antibodies in WNV Kunjin-infected U2OS cells. WNV capsid is shown in red (upper panel) and DDX55 is shown in green (middle panel). Merged images are shown with nuclear staining (Hoescht – in blue, lower panel)**. d**, Detection of DDX55 by western blotting using a DDX55-specific antibody following treatment with control (siCON) or two independent siRNAs targeting DDX55 (siDDX55-1, siDDX55-2). For **a-d**, all images are representative of two biologically independent experiments repeated with similar results.

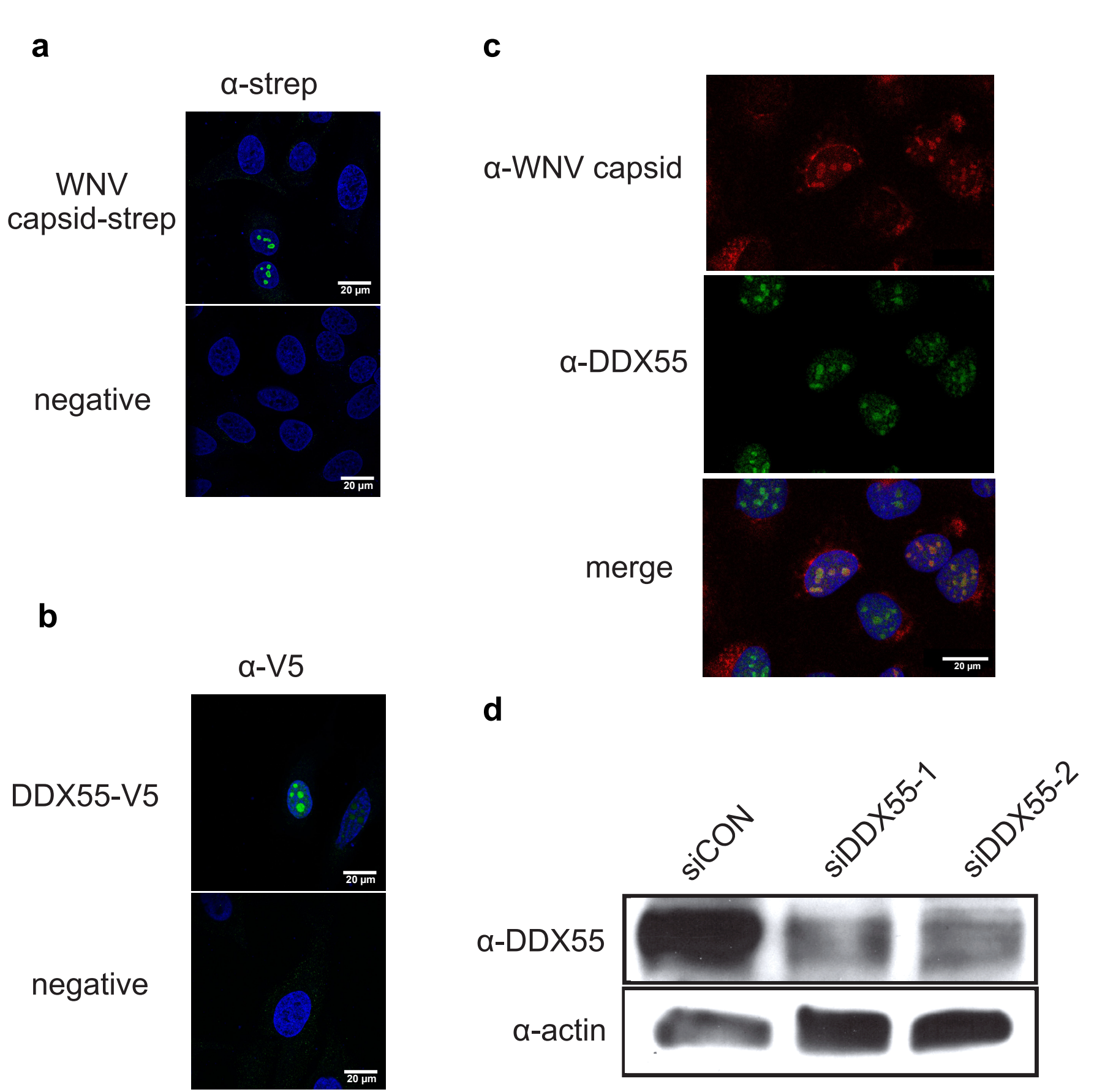

Supplementary Figure 4

Supplementary Figure 5: Enrichment of GO terms for individual baits. Heat map representing enriched KEGG Pathway, GO Biological Processes, GO Molecular Function, Reactome Gene Sets, Canonical Pathways and CORUM biological processes of the host factors interacting with indicated bait proteins. Results are derived from four biologically independent experiments. The colors represent statistical significance (-Log(P) value) as indicated by the accompanying scale. P-values were calculated based on accumulative hypergeometric distribution and the most statistically significant term within a cluster was chosen as the representative category for each cluster.

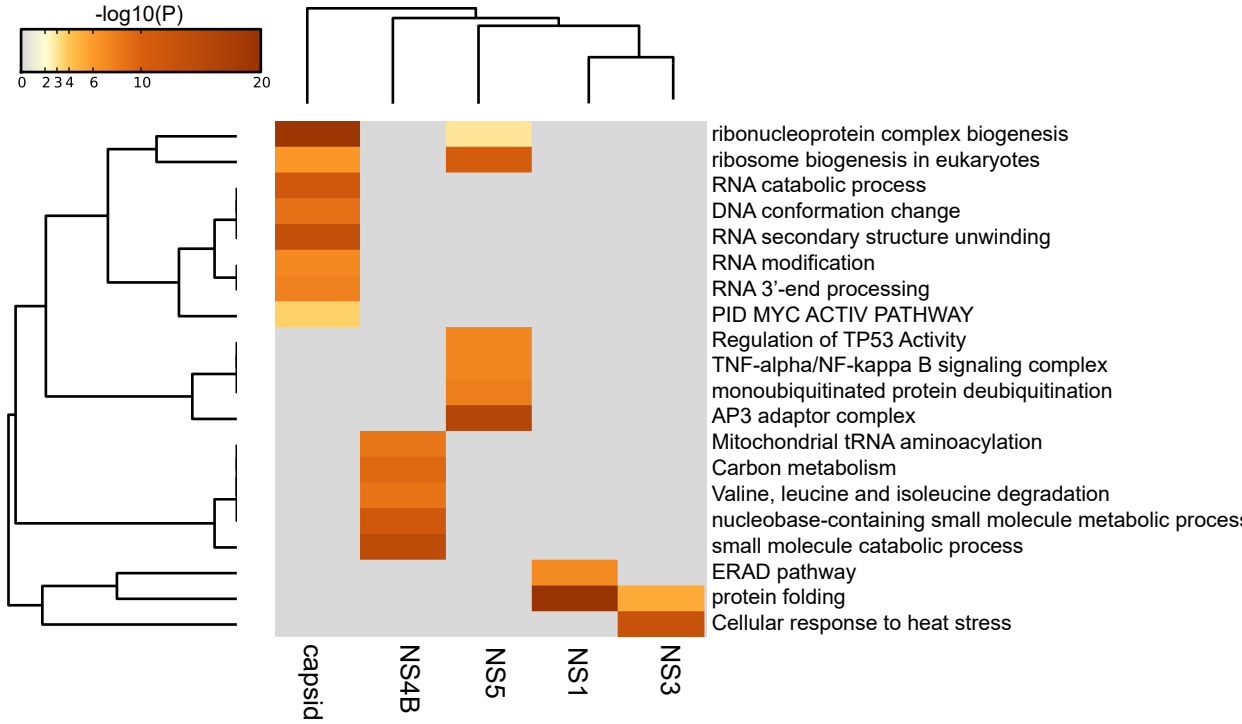

Supplementary Figure 5

Supplementary Figure 6: PYM1 knock-downs. a, Localization of native WNV capsid and native PYM1 using specific antibodies in WNV Kunjin-infected U2OS cells and uninfected controls. WNV capsid is shown in red (left panel) and PYM1 is shown in green (middle panel). Merged images are shown with nuclear staining (Hoescht – in blue, right panel)**.** Scale bar = 18µm. Images are representative of two biologically independent experiments repeated with similar results. **b**, Relative PYM1 RNA (PYM1/18S) following treatment with control (siCON) or two independent siRNAs targeting PYM1 (siPYM1-1, siPYM1-2). Shown is the mean±SE, n = three biologically independent experiments. Significance was calculated using an unpaired, two-tailed student's t-test and is indicated by *** $p < 0.0005$.

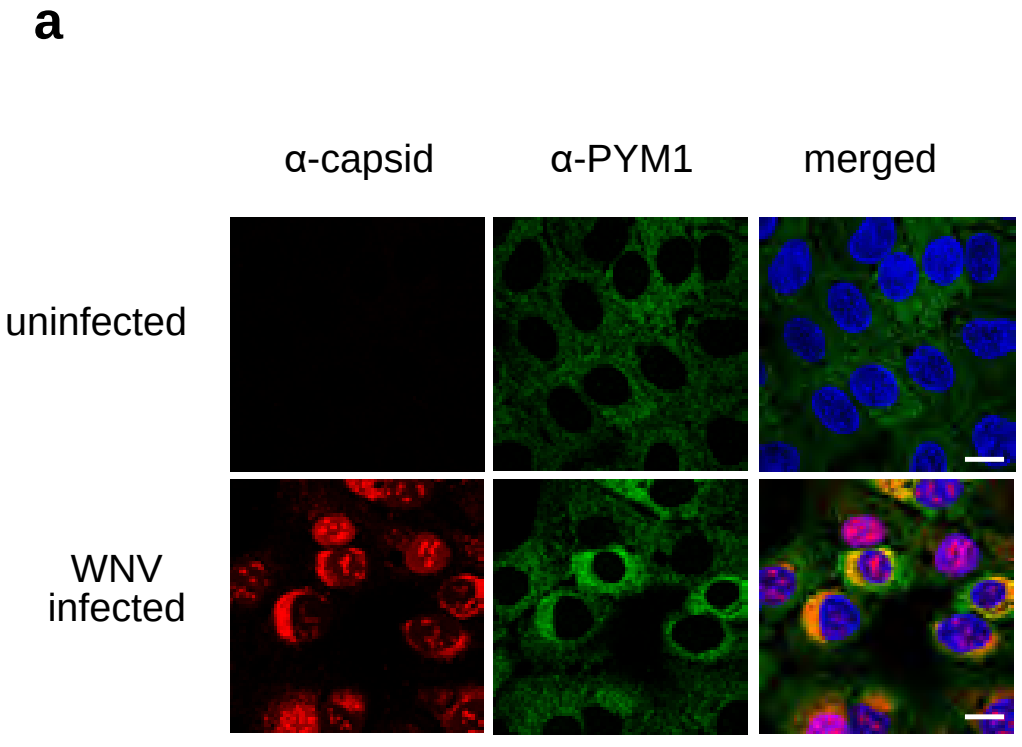

Supplementary Figure 6

Supplementary Figure 7: NMD and the EJC are antiviral and targeted by flaviviruses. a, U2OS cells were infected with the indicated viruses at MOI 10 and analyzed at the indicated time points. Two endogenous targets of the NMD mRNA surveillance pathway (CARS, left panel; ASNS, right panel) were analyzed by quantitative RT-PCR. **b**, A control RNA (LDHA) does not accumulate in flaviviral infection. Gene expression data (gene/18S) are normalized to uninfected controls. **c**, U2OS cells were treated with control (siCON) or PYM1-targeting siRNAs (siPYM1-1, siPYM1-2), infected with WNV at MOI 10 and analyzed at 24 hours post-infection. Two endogenous targets of the NMD mRNA surveillance pathway (SC35, left panel; GABARAPL1, right panel) were analyzed by quantitative RT-PCR. For **a-c**, shown is the mean±SE; n = three biologically independent experiments. Significance was calculated using an unpaired, two-tailed student's t-test and is indicated by * $p < 0.05$, ** $p < 0.005$, *** $p < 0.0005$.

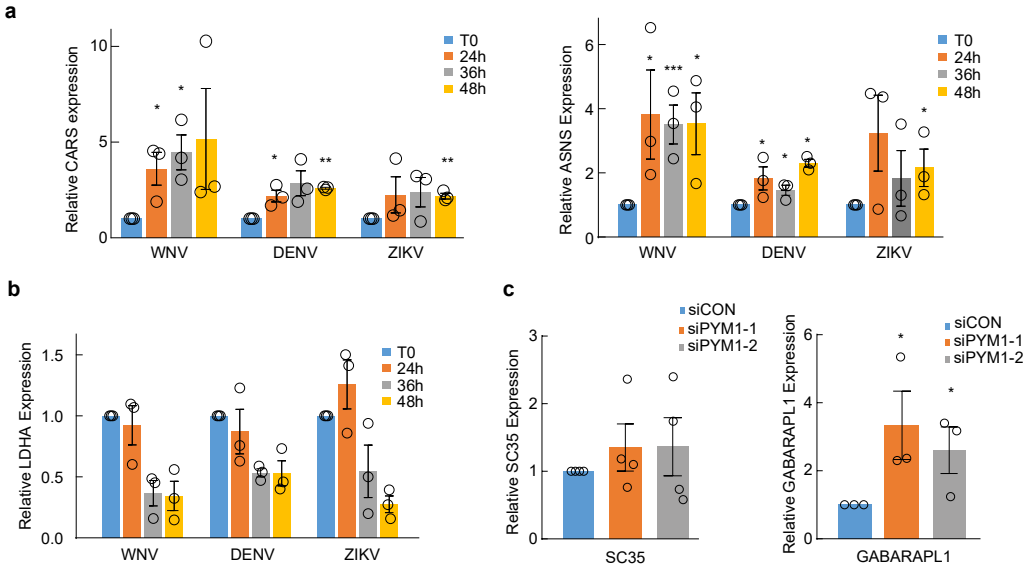

Supplementary Figure 7

Supplementary Figure 8. NMD is inhibited by flaviviruses through targeting of the EJC. a, Relative MAGOH RNA (gene/GAPDH) was measured in control cells (siCON) and MAGOH-depleted cells (siMAGOH-1, siMAGOH-2) (left panel). Relative SC35 RNA (gene/GAPDH) was measured in control cells (siCON) and MAGOH-depleted cells (siMAGOH-1, siMAGOH-2) (right panel). **b**, Relative UPF1 RNA (gene/18S) was measured in control cells (siCON) and UPF1-depleted cells (siUPF1-1, siUPF1-2) (left panel). Relative SC35 RNA (gene/18S) was measured in control cells (siCON) and UPF1-depleted cells (siUPF1-1, siUPF1-2) (right panel). For **a-b**, gene expression data is shown as the mean±SE; n = three biologically independent experiments. Significance was calculated using an unpaired, two-tailed student's t-test and is indicated by * $p < 0.05$, ** $p < 0.005$, *** $p < 0.0005$. **c**, Cellular fractionation experiments show the relative abundance of MAGOH, RBM8A and PYM1 in the whole cell lysate (WCL), cytoplasmic (Cyto), nuclear (Nuc), and membrane/organelle (Mem) fractions between control siRNA and PYM1-depleted (siPYM1) cells. Tubulin (cytoplasm), Lamin B1 (nucleus) and AIF (mitochondria) are shown as fractionation markers and loading controls. Results are representative of two biologically independent experiments repeated with similar results. **d**, The input PYM1, MAGOH and RBM8A for WNV RNA immunoprecipitations and the immunoprecipitated proteins using specific antibodies (labeled as Ab) and an IgG control antibody are shown by western blot. For PYM1, the light chain antibody is indicated by (*) (bottom panel). Results are representative of three biologically independent experiments repeated with similar results. **e**, The input PYM1, MAGOH and RBM8A for WNV RNA immunoprecipitations from siControl (siCON), PYM1-depleted (siPYM1) and MAGOH-depleted (siMAGOH) cells and immunoprecipitated RBM8A (IP) using an α-RBM8A antibody are shown by western blot. Results are representative of three biologically independent experiments repeated with similar results.

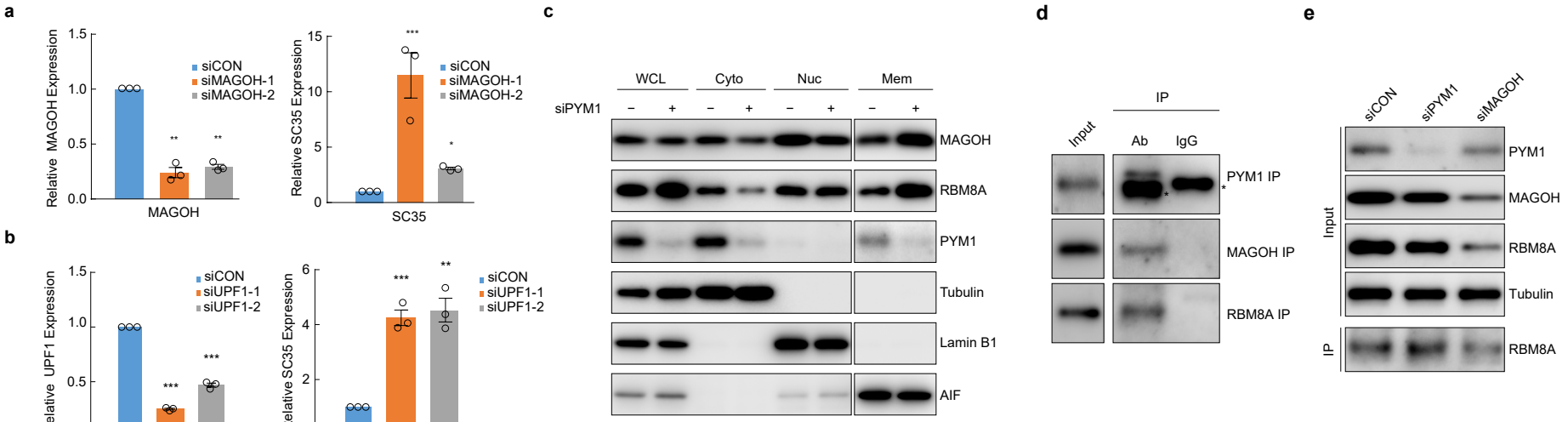

Supplementary Figure 8

Supplementary Figure 9: Model for PYM1, EJC proteins and NMD in flaviviral infection. The EJC complex (including RBM8A and MAGOH) associates with normal and PTC-containing host transcripts. RBM8A and MAGOH are removed from normal transcripts to allow translation and remain associated with PTC-containing transcripts to initiate nonsense-mediate decay. In WNV-infected cells, RBM8A (and possibly other EJC components) interact with WNV RNA, targeting viral RNA for degradation by the NMD machinery. This is subverted by West Nile virus capsid binding to PYM1, relocalizing RBM8A/MAGOH from the viral RNA into a membrane compartment. This results in reduced interaction of RBM8A/MAGOH to NMD-targeted host mRNAs and viral RNA, rescuing both from degradation by the NMD machinery.

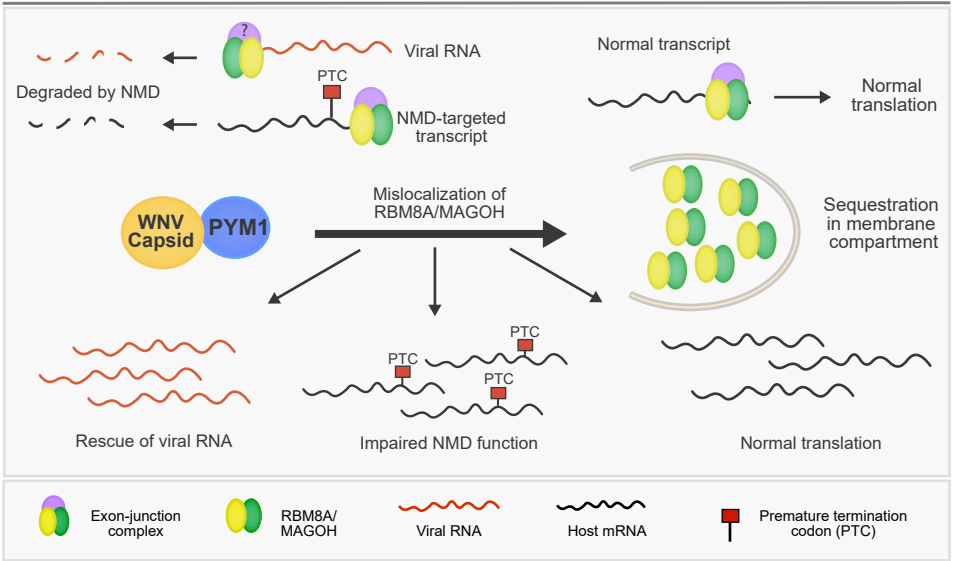

Supplementary Figure 9

Supplementary Figure 10. Unmodified western blot data. The raw data for all western blots are provided as unmodified images. The lanes that are relevant to the corresponding main text figure and the molecular weight markers are indicated.

Raw western blot images relating to Figure 3h

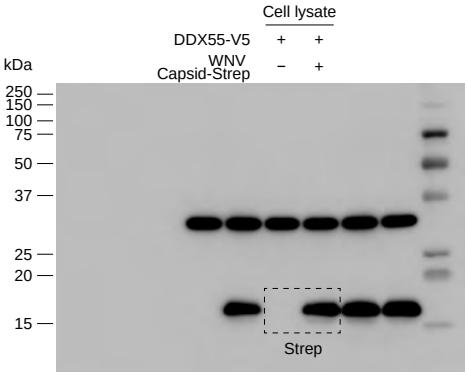

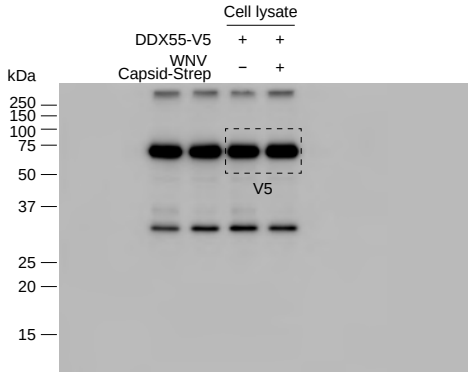

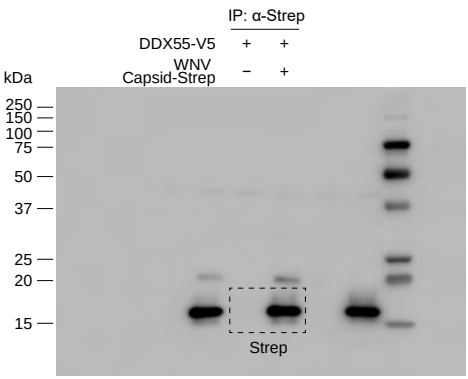

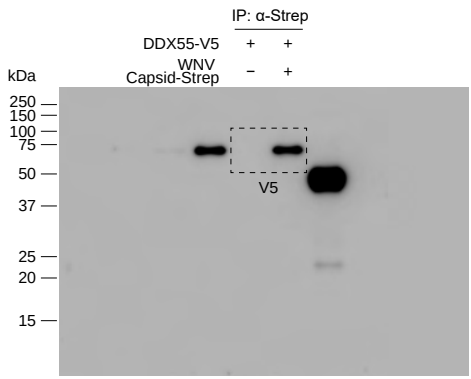

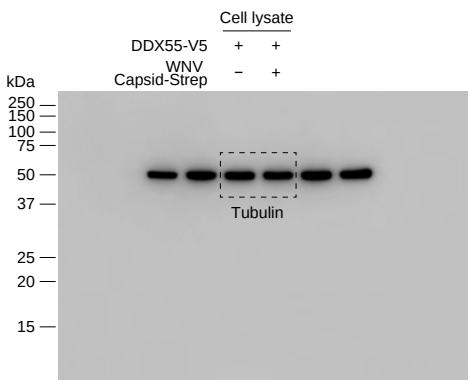

Supplementary Figure 10

Raw western blot images relating to Figure 5a

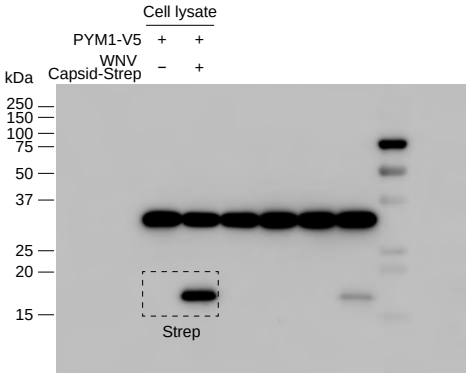

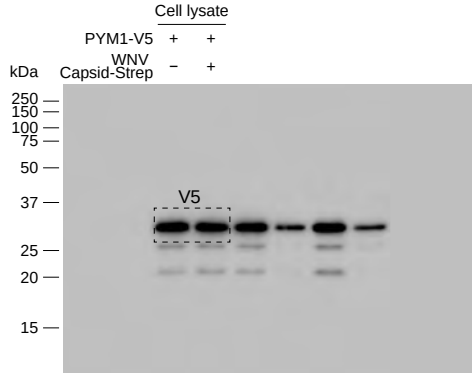

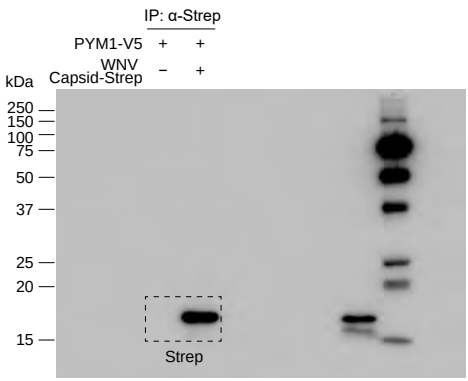

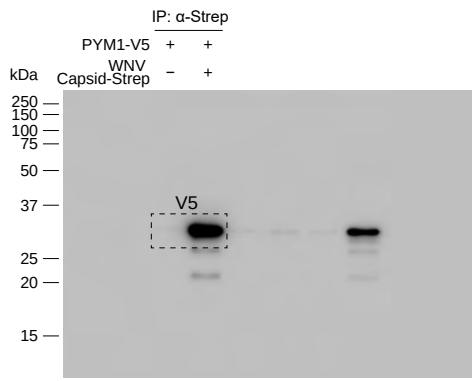

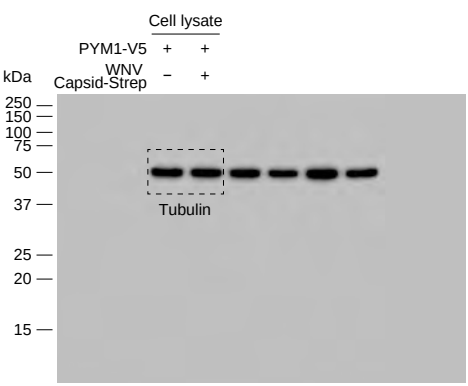

Supplementary Figure 10 continued

Raw western blot images relating to Figure 5b

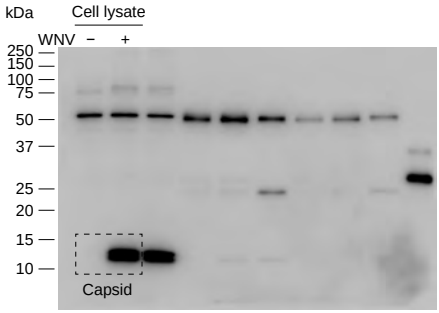

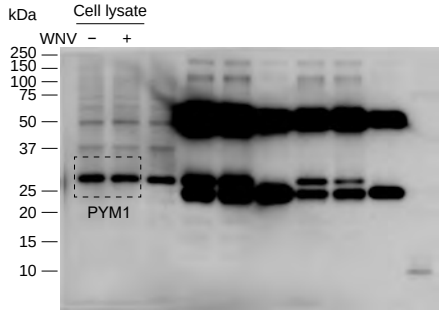

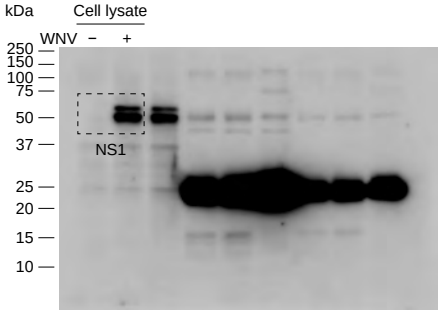

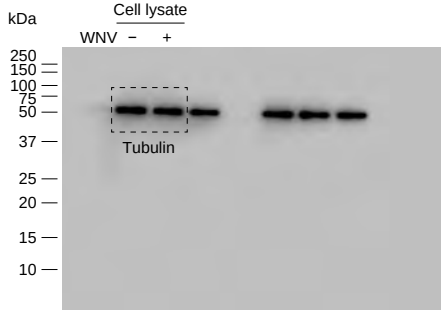

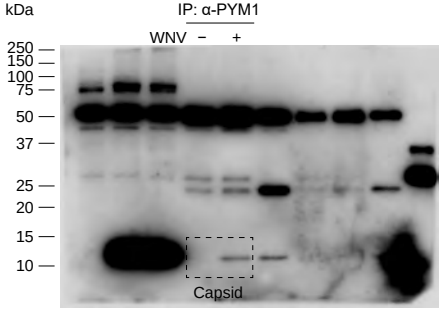

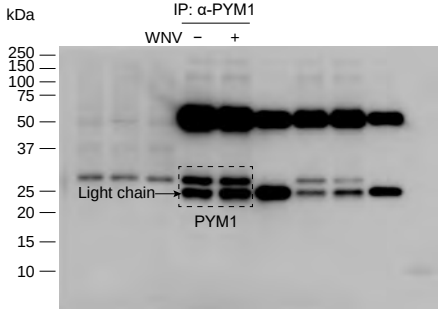

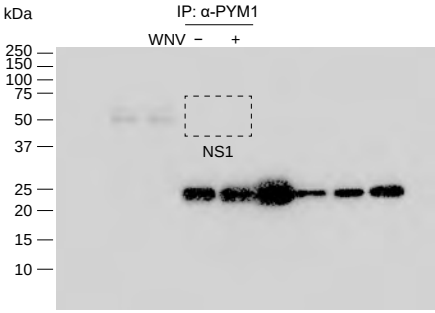

Supplementary Figure 10 continued

Raw western blot images relating to Figure 5e (left panel)

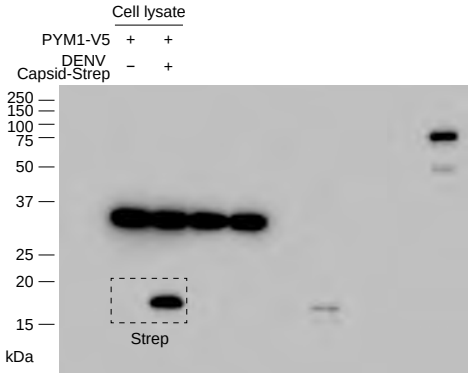

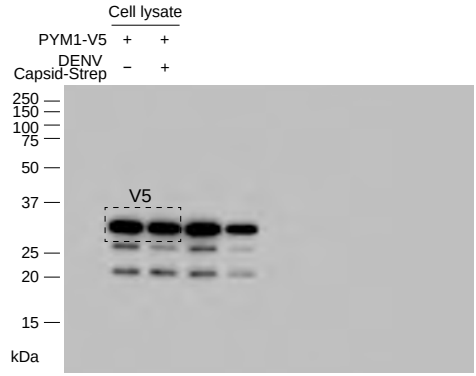

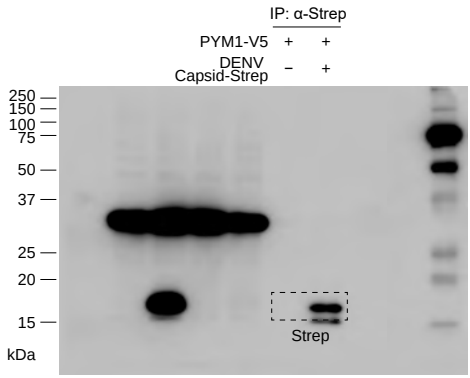

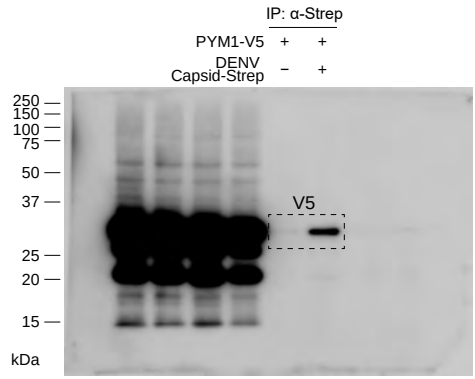

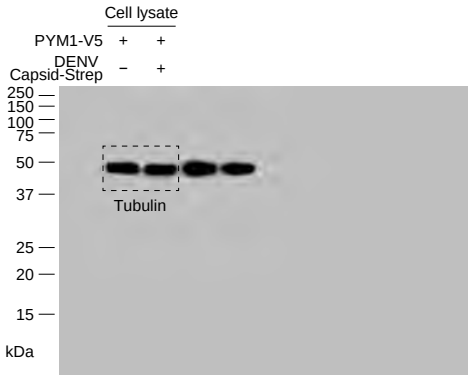

Supplementary Figure 10 continued

Raw western blot images relating to Figure 5e (right panel)

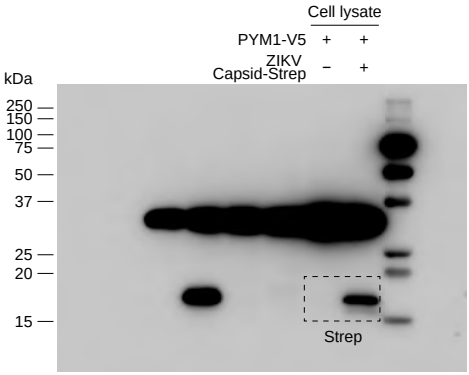

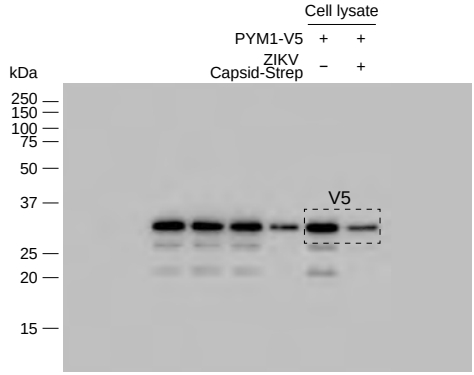

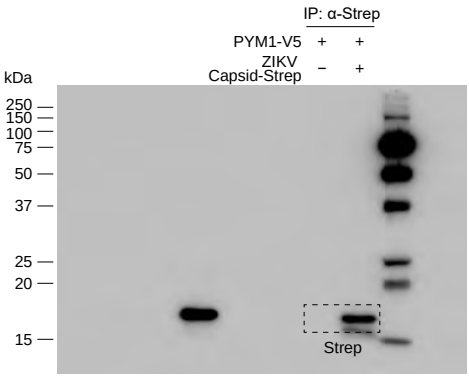

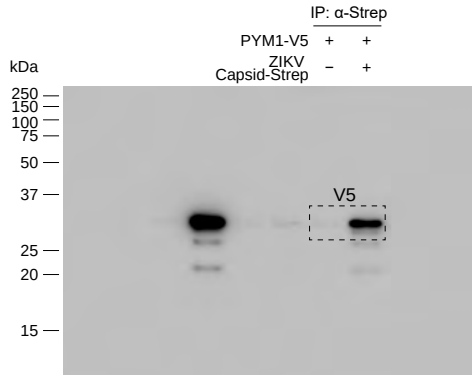

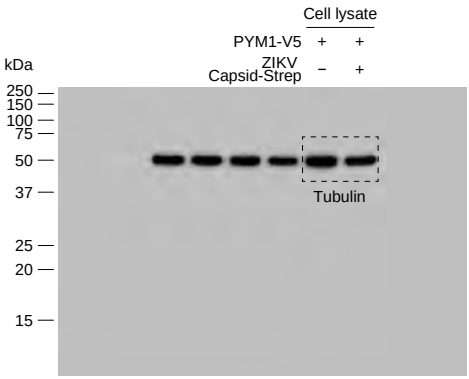

Supplementary Figure 10 continued

Raw western blot images relating to Figure 6d

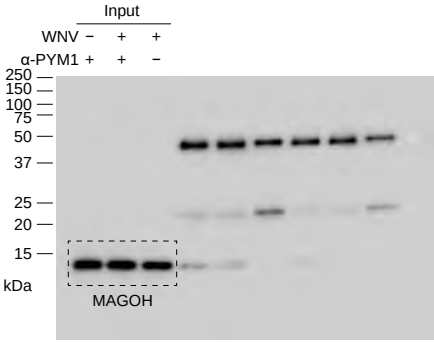

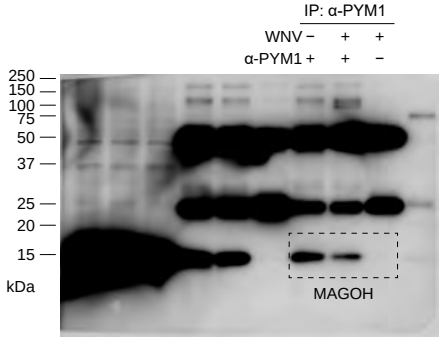

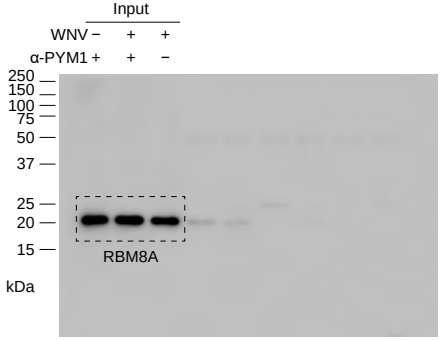

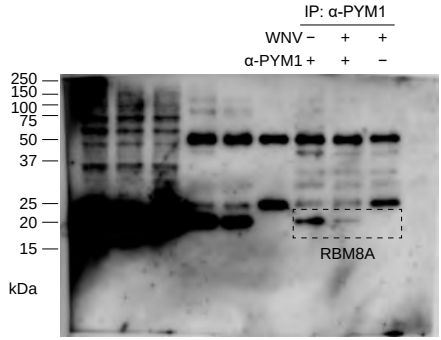

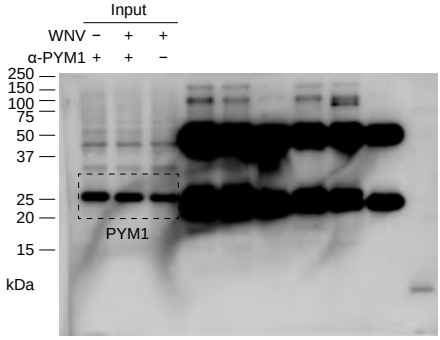

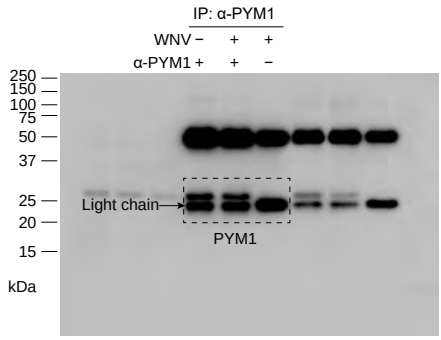

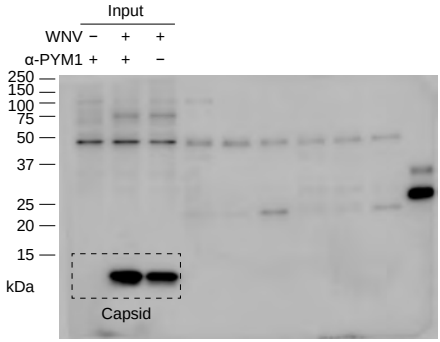

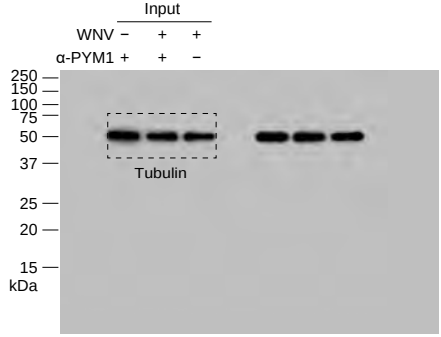

Supplementary Figure 10 continued

Raw western blot images relating to Figure 6e

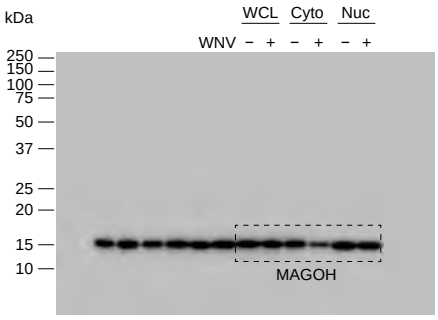

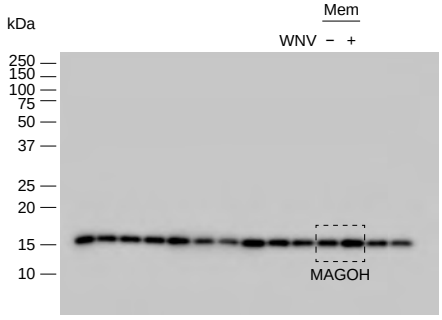

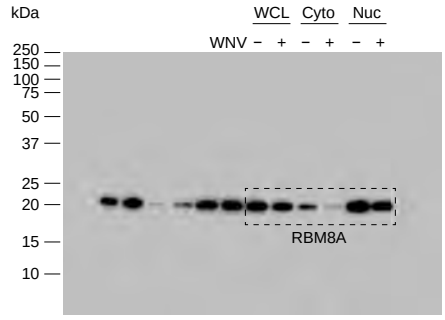

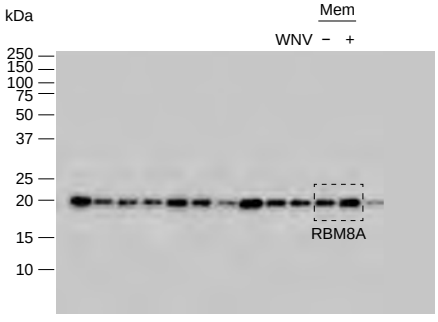

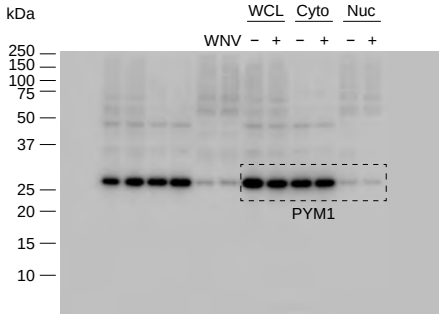

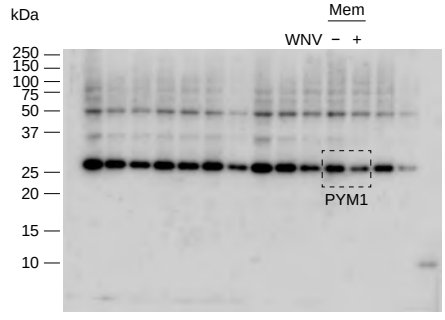

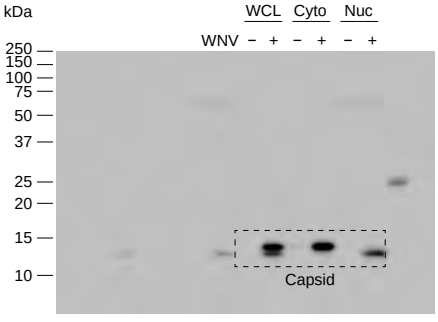

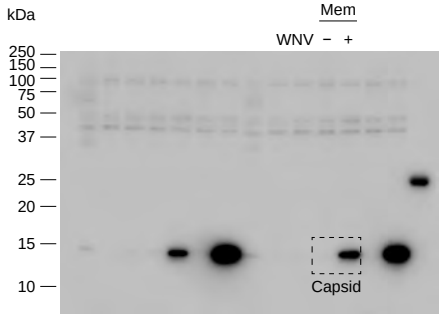

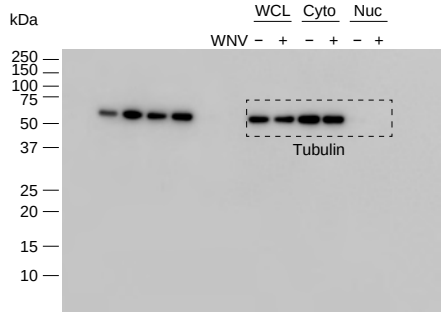

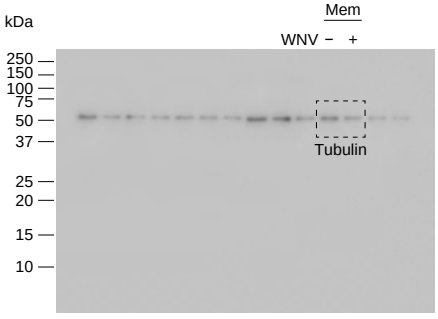

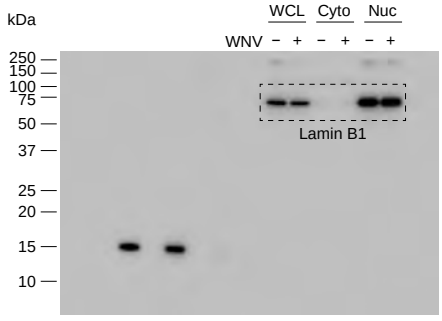

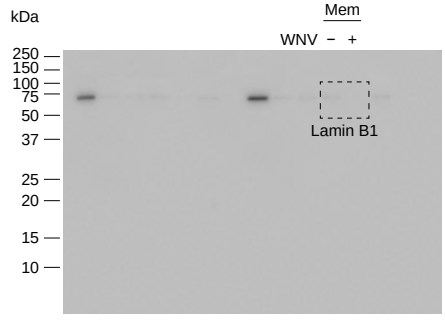

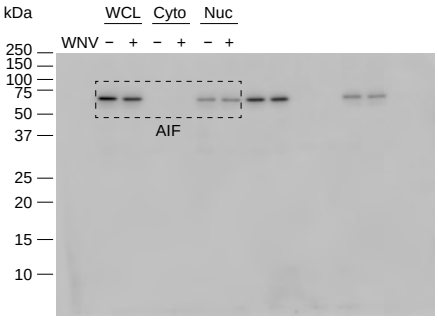

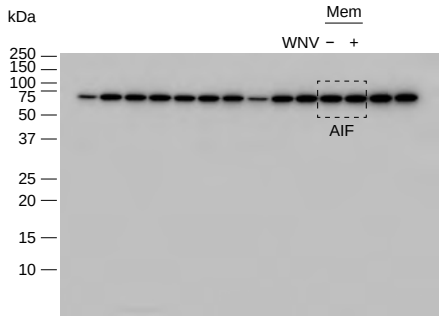

Supplementary Figure 10 continued

Raw western blot images relating to Supplementary Figure 1

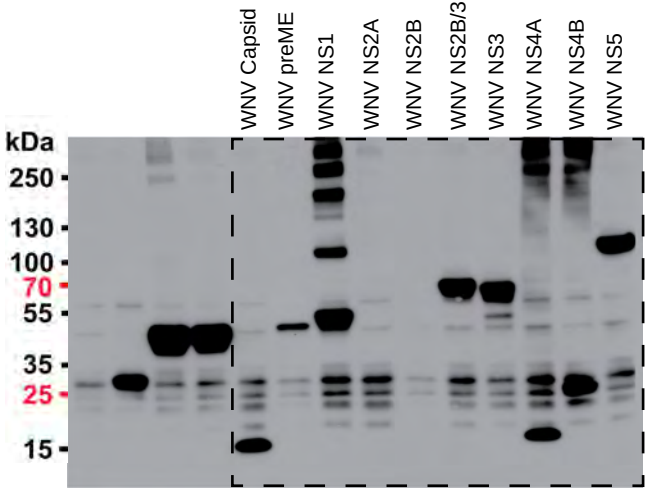

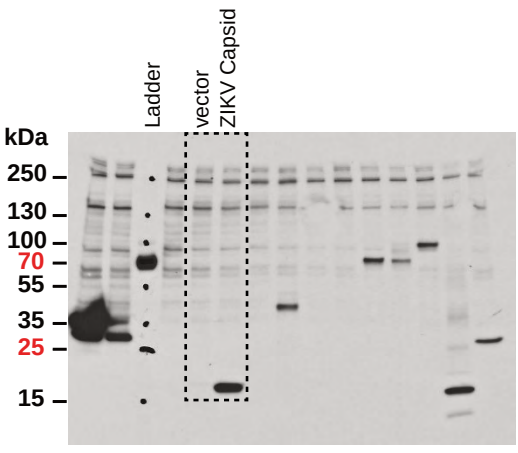

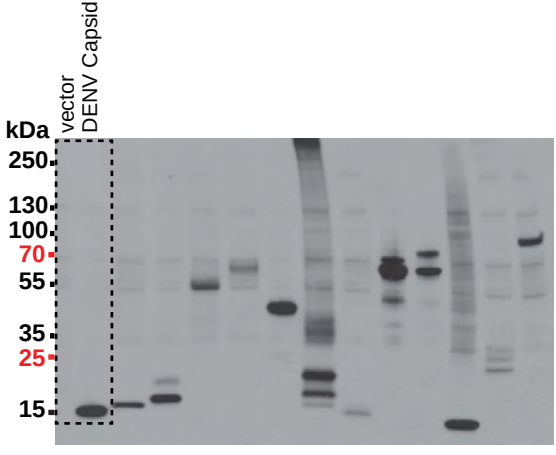

Supplementary Figure 10 continued

Raw western blot images relating to Supplementary Figure 4d

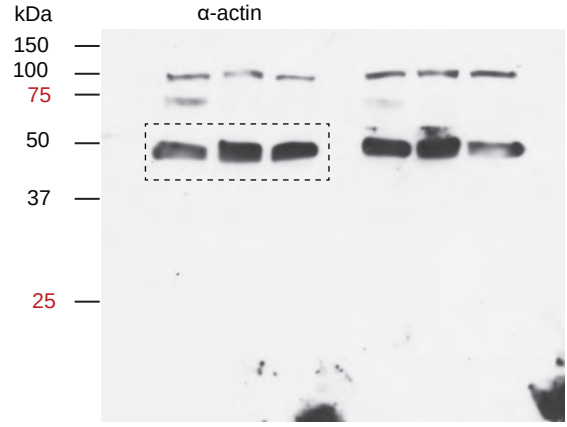

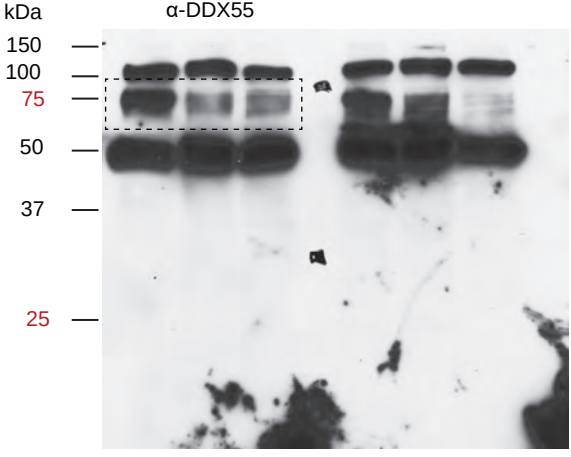

Supplementary Figure 10 continued

Raw western blot images relating to Supplementary Figure 8c

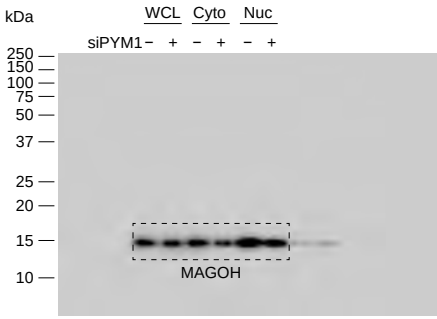

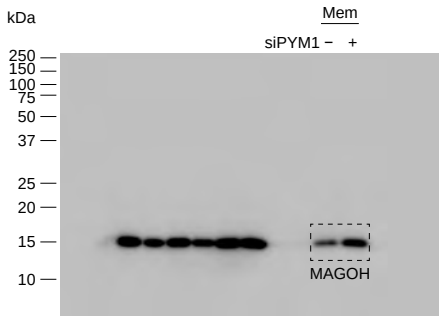

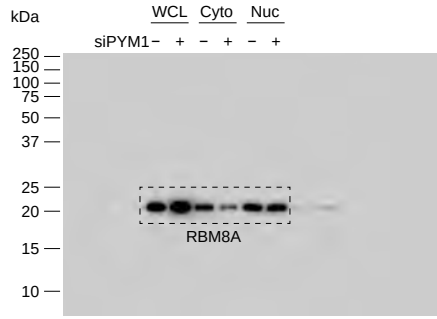

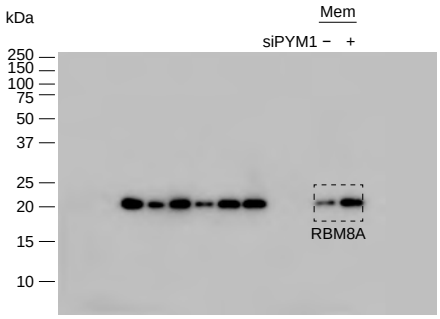

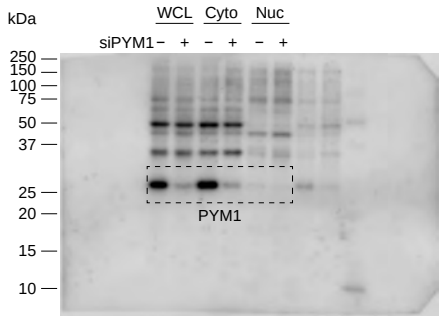

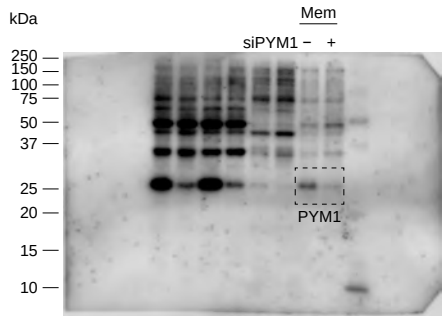

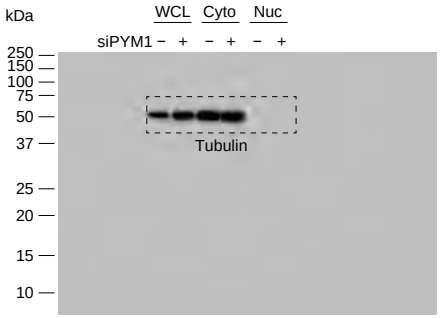

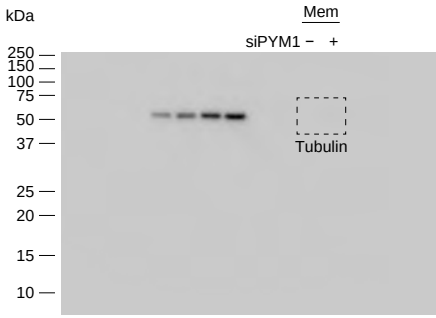

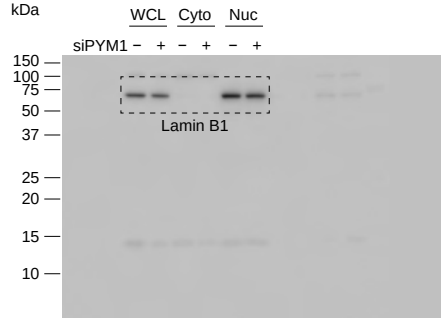

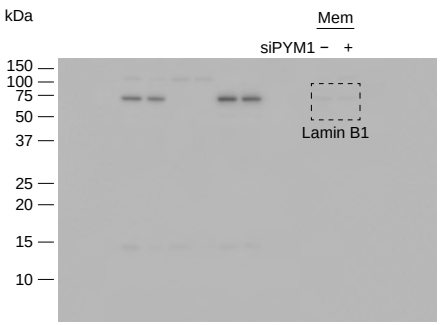

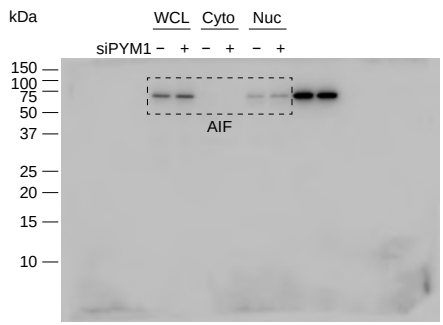

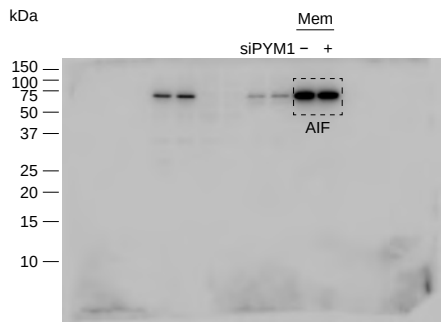

Supplementary Figure 10 continued

Raw western blot images relating to Supplementary Figure 8d

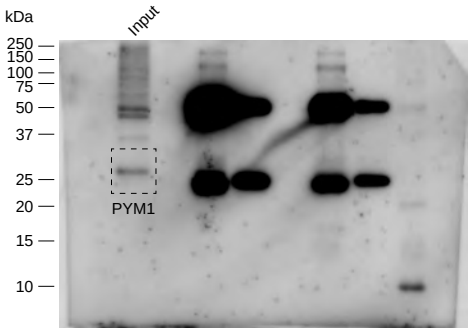

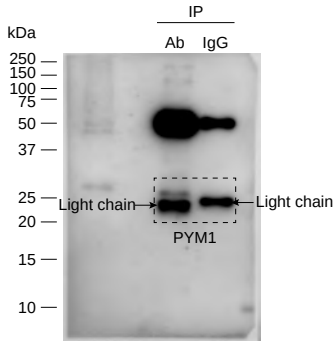

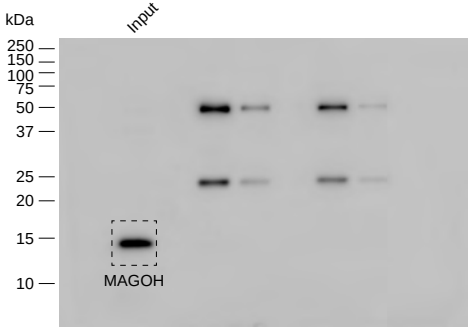

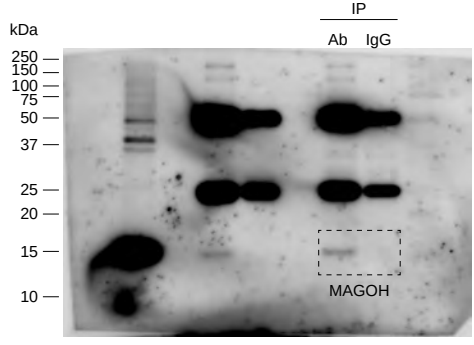

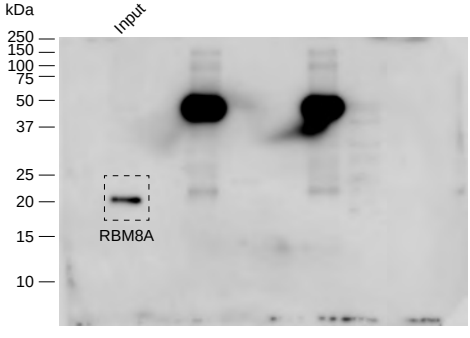

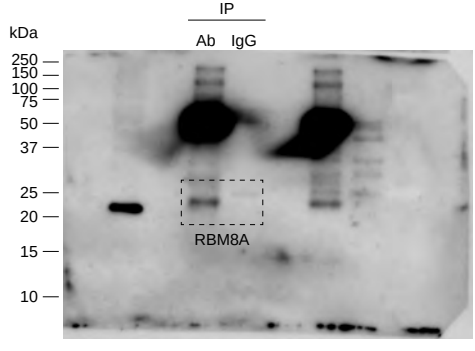

Supplementary Figure 10 continued

Raw western blot images relating to Supplementary Figure 8e

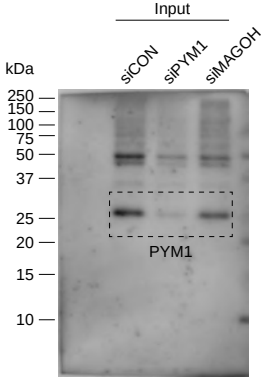

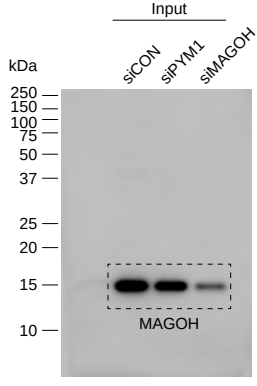

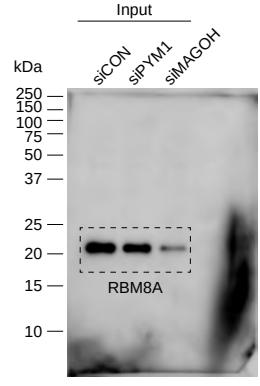

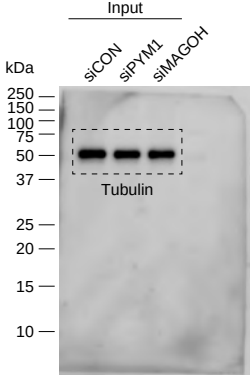

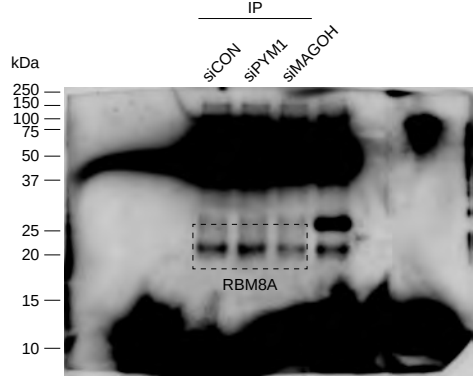

Supplementary Figure 10 continued

Supplementary Tables

Supplementary Table 1: WNV-interacting Proteins Identified by AP/MS. A summary of all MIST and COMPPASS scores for all interacting host proteins detected in HEK293T cells following immunoprecipitation with the indicated viral bait protein. Scores are derived from four biologically independent experiments.

Supplementary Table 2: High Confidence WNV-host Protein-Protein Interactions. A summary of all MIST and COMPPASS scores for host proteins above cut-offs included in the final interactome. Details on scoring parameters and cut-offs can be found in the Interactome Scoring and Visualization section of the Experimental Methods.

Supplementary Table 3: GO Enrichment for WNV Interactome. This data was generated using pathway and process enrichment analysis was carried out using the following ontology sources: KEGG Pathway, GO Biological Processes, GO Molecular Function, Reactome Gene Sets, Canonical Pathways and CORUM. All genes in the human genome were used as the enrichment background. Terms with p-value < 0.01, minimum count 3, and enrichment factor > 1.5 (enrichment factor is the ratio between observed count and the count expected by chance) are collected and grouped into clusters based on their membership similarities. P-values were calculated based on accumulative hypergeometric distribution and the most statistically significant term within a cluster was chosen as the representative category for each cluster. All analyses were derived from four biologically independent experiments and visualized using Metascape.

Supplementary Table 4: Overlap of WNV interactome with previous flavivirus AP-MS and genetic screens. WNV-interacting host proteins and WNV baits are listed for the overlap with flavivirus AP-MS studies (Tab 1, Overlap with proteomics studies) and genetic screens (Tab 2, Overlap with genetic studies). The PMID for all previously published studies is indicated.

Supplementary Table 5: Overlap of WNV Capsid Interactors with DENV and ZIKV Capsids. List of WNV capsid-interacting host proteins indicating interactions with WNV, DENV and ZIKV capsids. Additional tabs provide analyzed mass spectrometry results for interactions with DENV capsid (Tab 2) and ZIKV capsid (Tab 3).

Supplementary Table 6: GO Enrichment for WNV Capsid Interactors. Pathway, process and localization enrichment analysis was carried out on all capsid-interacting proteins with the following ontology sources: KEGG Pathway, GO Biological Processes, GO Molecular Function, Go Cellular Components, Reactome Gene Sets, Canonical Pathways and CORUM. All genes in the human genome were used as the enrichment background. Interactors in each category list for each bait protein with values indicating significance are shown. P-values were calculated based on accumulative hypergeometric distribution and the most statistically significant term within a cluster was chosen as the representative category for each cluster. All analyses were derived from four biologically independent experiments and visualized using Metascape. Details on enrichment analysis can be found in Methods.

Supplementary Table 7: Enrichment of WNV-Interactor Localization and GO Terms for Individual WNV Bait Proteins. Pathway and process enrichment analysis was carried out on the host interactor set for each of the WNV bait proteins with the following ontology sources: KEGG Pathway, GO Biological Processes, GO Molecular Function, Go Cellular Components, Reactome Gene Sets, Canonical Pathways and CORUM. Interactors in each category list for each bait protein with values indicating significance are shown. Cellular component membership for interactors of each WNV bait protein are shown in the following cellular component categories: cytoplasm, Golgi apparatus, endoplasmic reticulum (ER), mitochondria, nucleus and nucleolus.

All genes in the human genome were used as the enrichment background. Interactors in each category list for each bait protein with values indicating significance are shown.

Supplementary Table 8: Complete RNAi Screening Results (Robust Z-scores). The list of all host protein interactors and associated WNV bait proteins chosen for the RNAi screen. Summary of the RNAi screen data generated for all candidates after excluding factors that resulted in toxicity upon depletion. Shown are the average Robust Z-scores for two biologically independent experiments for infections in WNV, DENV and ZIKV.

Supplementary Table 9: siRNAs used in this study.

Supplementary Table 10: qPCR primers used in this study.

Supplementary Table 11: Complete table of precise p-values for all statistical analyses.